

RSC Advances



This is an *Accepted Manuscript*, which has been through the Royal Society of Chemistry peer review process and has been accepted for publication.

Accepted Manuscripts are published online shortly after acceptance, before technical editing, formatting and proof reading. Using this free service, authors can make their results available to the community, in citable form, before we publish the edited article. This *Accepted Manuscript* will be replaced by the edited, formatted and paginated article as soon as this is available.

You can find more information about *Accepted Manuscripts* in the [Information for Authors](#).

Please note that technical editing may introduce minor changes to the text and/or graphics, which may alter content. The journal's standard [Terms & Conditions](#) and the [Ethical guidelines](#) still apply. In no event shall the Royal Society of Chemistry be held responsible for any errors or omissions in this *Accepted Manuscript* or any consequences arising from the use of any information it contains.

Multimodal Theranostic Nanomaterials Derived from Phthalocyanine-based Organic Salt

Susmita Das^{1,3,*}, Paul K. S. Magut¹, Lijie Zhao¹, Farhana Hasan,¹ Amar B. Karki², Rongying Jin², and Isiah M. Warner^{1,*}

¹Department of Chemistry, Louisiana State University, Baton Rouge, LA-70803, USA

²Department of Physics, Louisiana State University, Baton Rouge, LA-70803, USA

³Department of Materials Science, Indian Association for the Cultivation of Science, Jadavpur, Kolkata-700032, WB, India

*Corresponding Authors' - email: ssmtdas@gmail.com, mssd2@iacs.res.in; iwarner@lsu.edu

Abstract

Emerging concepts of theranostics have led to development of numerous multifunctional nanomaterials using various synthetic approaches. Herein, we report a simplistic approach towards design of an Iron(III) phthalocyanine based pH responsive-magnetic-fluorescent nanoparticles for combined multimodal diagnosis and possible site selective therapy. Transmission electron micrographs (TEM) revealed distinct spherical (~25-35 nm) nanoparticles, constituting a significantly stable nanodispersion which resulted from an appreciably high positive zeta potential (+21 mV) at pH 7.4. A transition in magnetic behavior of these nanoparticles (diamagnetism in bulk, paramagnetism in nanoparticles at room temperature and superparamagnetism at 200 K), in combination with acidic pH responsive loss of spherical shape, pH responsive release of chemotherapeutic agents in vitro, and confocal fluorescence microscopic images suggest potential utility of these materials as multimodal theranostic agents. A novel approach for design of multifunctional theranostic devices, as demonstrated in this study, represents an important development in this area of scientific research.

Keywords: Nanotheranostic, Drug delivery, pH responsive, Paramagnetic, Organic salt

Introduction

Design of nanometer sized vehicles for stimuli responsive delivery of therapeutic agents is extremely important with respect to development of techniques for non-invasive treatment of diseases. In recent years, tremendous effort has been made towards development of engineered theranostic nanomaterials with multifunctional and multimodal characteristics that are capable of concomitant therapy and diagnosis.¹⁻⁴ This is because nanodimensional materials interact more effectively with biological systems at cellular level, thereby allowing early detection of diseases.¹⁻⁴ Nanomaterials also enabling higher drug loading due to high surface area-to-volume ratio.¹⁻⁴ Drug encapsulated nanomaterials typically exhibit prolonged half lives due to enhanced circulation times within the body, as compared to early excretion of free drug molecules before achieving desired activity.⁵ Additionally, incorporation of target specificity to these nanoscale delivery vehicles enables administration of lower doses, thereby reducing associated side-effects.^{6,7}

Development of multifunctional theranostic nanoparticles require judicious fabrication of materials through integration of different functionalities such that all properties are preserved upon nanoformulation. Several strategies have been investigated thus far towards synthesis of multifunctional nanoparticles.⁸⁻¹⁷ For example, surface modification of a magnetic nanoparticle with site specific ligands via covalent attachments have been used for incorporation of desired multiple functionalities. Conjugation of a protein or antibody adds target specificity to such magnetic nanoparticles, thereby affording better contrast in MRI which allows improved distinction between the site of interest and the surrounding region.^{9,10} Target specificity can also be incorporated by attaching a stimuli responsive element such as pH^{13, 14} or temperature sensitive polymers¹⁴ to magnetic nanoparticles. pH being an important indicator of several

pathological conditions, pH responsive nanoparticles are intensively investigated for both diagnosis and site specific drug delivery.^{13,14} In such applications, fluorescence is often used for tracking activity of nanoparticles as well monitor the progress of the medical process.^{12, 13} Conjugation of fluorescent behavior with magnetic nanomaterials has been performed using several techniques.¹⁵ For example, fluorescent nanoparticles or molecules are generally coupled with magnetic nanoparticles through electrostatic or covalent linkage. Alternatively, fluorescent nanoparticles are synthesized within the core of magnetic nanoparticles, which are generally referred to as core-shell nanoparticles.^{15,17} However, nanoparticles synthesized using such techniques usually exhibit low fluorescence quantum yields (QY) or degradation of fluorescence QY due to loss of ligands from their surface.⁸ It becomes even more challenging to retain all the desired properties when a third functionality such as target specificity is incorporated into such nanoparticles due to the increased complexity of the microenvironment. Thus, obtaining multifunctional nanotheranostic devices with satisfactory performance in the actual cellular environment is quite difficult. Besides, nearly all variations of multifunctional nanomaterials reported thus far involve multistep, sophisticated, and elongated synthetic approaches for incorporation of each functionality leading to more expensive end products. Therefore, development of new materials and novel simplistic strategies for development of such devices is essential.

In this study, we report on an extremely facile approach to tailoring an existing molecule for demonstration of improved functionality upon nanoformulation, which allows combined stimuli responsive therapeutic and diagnostic applications. These multifunctional theranostic nanomaterials are based on iron phthalocyanines and combine fluorescent, magnetic as well as stimuli responsive properties. Iron(III)phthalocyanine has previously been used to coat surfaces

of Fe₂O₃ nanoparticles in order to obtain better dispersion in organic solvents, as well as to increase their antioxidant properties.¹⁸ Derivatives of this compound have also been used to design multilayered electrodes for use as resistive switching memory.¹⁹ Although phthalocyanines and phthalocyanine conjugated nanoparticles have been widely investigated for applications in photodynamic therapy,²⁰ iron phthalocyanines are not known to be used for such purposes. Besides, in all the above mentioned studies, metal phthalocyanines have been used in combination with other materials, primarily to improve redox properties.^{19, 20} However, to the best of our knowledge, nanomaterials derived directly from Iron(III)phthalocyanine or derivatives, as well as the influence of these materials on magnetic properties contributed by its metal ion core have not been previously explored. In addition, the use of Iron(III) phthalocyanine or its nanomaterials for therapeutic or diagnostic purposes has not been reported to date.

Herein we demonstrate a one step synthesis of an organic salt ([Ptc][DC] derived from Iron(III)phthalocyanine chloride ([Ptc][Cl] and a bile salt, sodium deoxycholate (NaDC), followed by nanoparticle formation through reprecipitation. Efficacy of these nanoparticles was examined for theranostic applications. The selective pH responsive drug delivery properties of these nanomaterials to cancer cells, the paramagnetic behavior as well as fluorescence imaging characteristics were established. Significantly high biocompatibility of this new class of nanomaterials place them as good competitors to existing theranostic nanoparticles.²¹⁻²³

Results and Discussions

In this study, ionic liquid chemistry is applied for incorporating various functionalities into a given compound using a simple materials design. The molecular design of the salt [Ptc][DC] was implemented with the idea that the Fe(III) core of phthalocyanine would

contribute magnetic properties and deoxycholate counteranion would impart pH sensitive properties. In addition, the strong absorption of phthalocyanine in the near infrared (NIR) and visible regions would also contribute to the optical properties of these materials.

Effect of pH on [Ptc][DC] nanoparticles

Examination of transmission electron micrographs (TEM) of the [Ptc][DC] nanoparticles revealed formation of distinct spherical particles of average size $\sim 25\text{-}35$ nm at pH 7.4 (Figure 1). The nanoparticle formation was primarily driven by self-assembly through hydrophobic, as well as $\pi\text{-}\pi$ interactions between individual [Ptc][DC] units. TEM micrographs revealed distinctly separate [Ptc][DC] nanoparticles and their stability in the colloidal state was further supported by their high positive zeta potential (+21.6 mV) value. However, at an acidic pH (pH 6), the nanoparticles were observed to coalesce (Figure 1) and lose their distinct shapes. Such pH sensitive behavior was ascribed to the presence of the deoxycholate counteranion. This counteranion has a pKa value near pH 6.8²⁴ suggesting protonation of the counteranion below this pH. Thus at pH 6, as expected from the molecular design, [Ptc][DC] decomposes leading to destabilization of the nanoparticles.

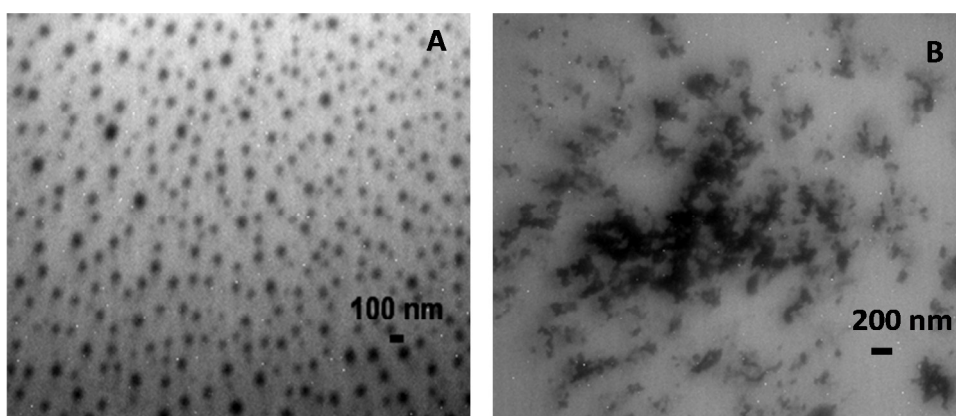


Figure 1: TEM micrographs of [Ptc][DC] nanoparticles respectively at (A) pH 7.4, (B) pH 6.

Destabilization of these nanoparticles at an acidic pH emphasizes on the utility of these nanoparticles for pH responsive and target specific drug delivery to cancerous cells. The appreciable stability of the nanoparticles at the physiological pH as suggested by the high positive and constant zeta potential value as a function of time indicated the appropriateness of these nanoparticles as stable drug carriers. Besides, the positive zeta potential of these nanoparticles should facilitate adsorption on or penetration into negatively charged cancer cell membranes²⁵ which will be an additional benefit for delivery of therapeutic agents.

Magnetic Properties of [Ptc][DC] Nanoparticles

Magnetism is one of the properties that have been widely exploited in nanomaterials for biomedical applications.²¹⁻²³ In this study, magnetic properties of both the bulk material and the lyophilized [Ptc][DC] nanoparticles were investigated. Field scans at a given temperature, as well as temperature scans at a given field were performed. Figure 2a is a plot of the field dependence of magnetization (M) at 300 K for bulk [Ptc][DC]. Note that M initially increases with increasing field, then decreases after reaching a maximum near ~ 100 Oe, and changes sign from positive at $H < 100$ Oe to negative at $H > 100$ Oe suggesting mostly diamagnetic behavior of bulk [Ptc][DC]. This behavior also indicates that magnetic interactions in bulk [Ptc][DC] are highly field dependent. In contrast, the [Ptc][DC] nanoparticles exhibit linear field dependence of magnetization between -7 and +7 Tesla as shown in Fig. 2b. Such behavior suggests paramagnetic interactions for these nanoparticles at 300 K. Interestingly, the magnetic susceptibility χ measured at 0.2 T shows little temperature dependence above ~ 60 K, as plotted in Figure 2c. While constant susceptibility usually suggests a small spin contribution, the nonlinear M vs. H curve obtained at 200 K (Fig. 2d) is indicative of superparamagnetic (S-shaped) behavior of [Ptc][DC] nanoparticles.¹⁴ Thus, our studies reveal an interesting transition

in magnetic behavior from [Ptc][DC] bulk to [Ptc][DC] nanoparticles which is attributed to enhanced phase coherence of magnetic dipoles within these nanomaterials, as compared to the bulk material.¹⁴ Magnetic nanoparticles generally possess an inherent tendency to agglomerate and are rapidly cleared by macrophages of the mononuclear phagocyte system upon intravascular administration.^{13, 14} Therefore, several efforts have been made to prevent nanoparticle agglomeration at physiological pH through surface modification, while considering non-toxicity of these particles besides other factors.^{26, 27} Thus, the highly stable nanoparticle dispersions obtained in our case at pH 7.4 without any surface modification is considered an inherent characteristics of these materials. Most of the pH responsive nanoparticles reported till date are generally obtained using polymeric materials.³ Therefore, design of pH responsive nanomaterials using a simple molecular system is viewed as an important improvement towards development of stable magnetic nanodispersion.

In addition, the effect of size of the nanoparticles on magnetic properties was also investigated (SI). It was observed that with increase in nanoparticle size (Figure S2), the magnetization increased (Figure S3) by nearly an order of magnitude from the smallest (15-20 nm) to the largest (50-65 nm) size. The increase in magnetization with size suggested the existence of a single magnetic domain in the studied size range. Size dependent variation of magnetic properties are well known for iron oxide nanoparticles and is attributed to the alteration in magnetic interactions with change in size.²³ These observations recommend substantial potential of [Ptc][DC] nanoparticles for applications in diagnosis and therapy as discussed earlier.

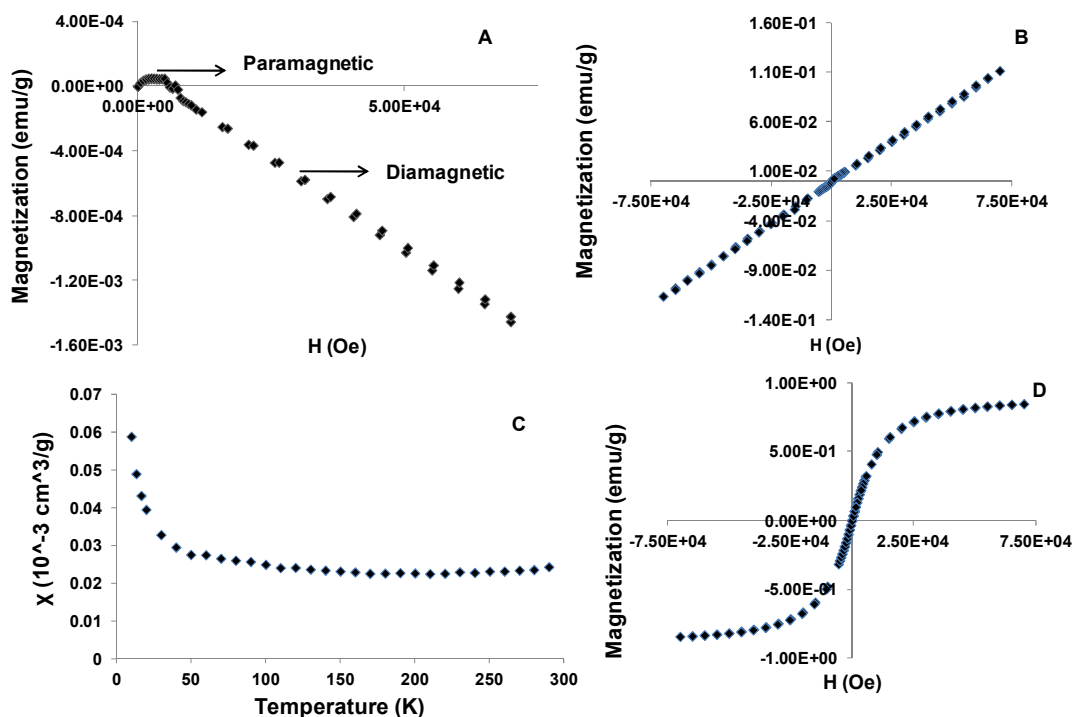


Figure 2: Magnetic properties of [Ptc][DC] (A) bulk M vs H at 300 K, (B) nanoparticles M vs H at 300 K, (C) nanoparticles χ vs T at 0.2 Tesla and (D) nanoparticles M vs H at 200 K.

pH Dependent Spectral Properties of [Ptc][DC] nanoparticles

Conjugation of fluorescence characteristics with pH responsive and magnetic properties into single material will enable target specific drug administration with multimodal diagnosis. Examination of the spectral properties (Figure 3) of [Ptc][DC] nanoparticles in an aqueous medium (buffer pH 7.4) reveal the presence of two characteristic bands of phthalocyanines viz. the intense and broad B-band lying in the UV region and the relatively less intense Q-band lying in the near infrared region (NIR) peaking at ~ 718 nm. At pH 6, a bathochromic shift of 60 nm was observed in the NIR region of the absorption spectra whereas in the UV region the absorption spectrum appeared to be the same with reduced absorbance value. These changes might be attributed to dissociation of the salt at this pH thereby altering its immediate

microenvironment. Shift in Q-band in the absorption spectra of phthalocyanines has been observed for substituted metal phthalocyanines in comparison to the unsubstituted compounds.²⁸ Measurement of steady-state fluorescence of these nanoparticles at the physiological pH value, produced a broad fluorescence emission in the visible region with a peak centered at ~500 nm using an excitation wavelength of 400 nm. However, no fluorescence emission was observed in the NIR region corresponding to absorption at 718 nm. This observation is in agreement with the literature which supports our observation of no NIR fluorescence for Fe phthalocyanines due to possible quenching by the paramagnetic metal ion present in the phthalocyanine core.²⁹ A slight quenching in fluorescence emission was encountered at pH 6 with the peak position remaining the same. This observation was in parity with the absorption peak in UV region whose position also remained unaffected by the change of pH. The fluorescence quantum yield of the nanoparticles was measured to be 0.03 for excitation at 400 nm. The fluorescence emission in the visible region implies towards the possible utility of these materials for simultaneous fluorescence imaging in conjunction with stimuli responsive drug delivery.

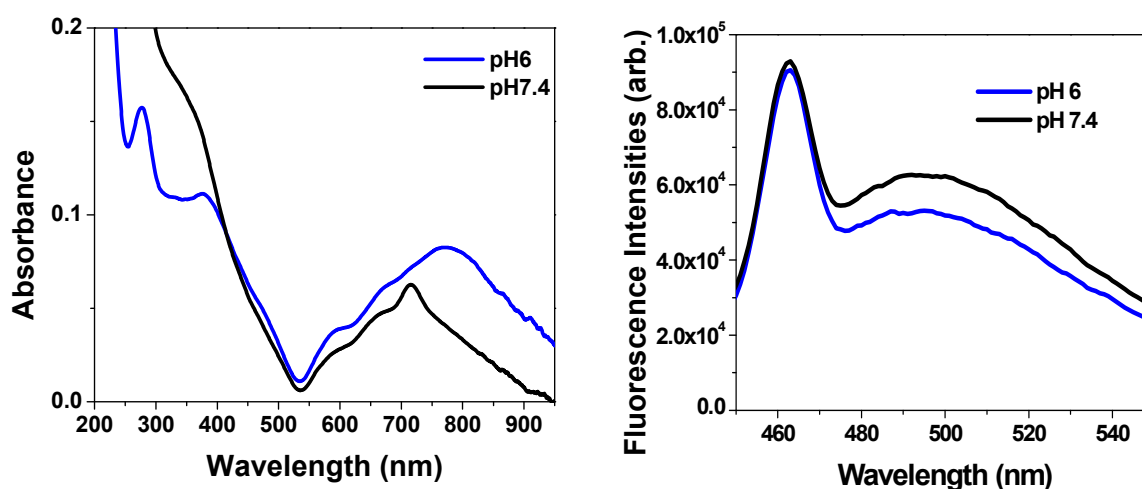


Figure 3: (A) Absorption spectra, (B) Fluorescence emission spectra ($\lambda_{\text{ex}}=400$ nm) of [Ptc][DC] nanoparticles (20 μM) with varying pH.

[Ptc][DC] nanoparticles as pH responsive carriers of therapeutic agents

The difference in extracellular pH of cancerous tissues in comparison to normal tissues has been taken advantage for design of drug delivery systems that undergo physical or chemical changes in response to altered pH conditions. Thus, the pH sensitive response of [Ptc][DC] nanoparticles was further investigated in order to examine its potential application for pH responsive release of therapeutic agents. A chemotherapeutic drug, doxorubicin, was encapsulated into [Ptc][DC] nanoparticles using the procedure described in our experimental section. The lyophilized drug encapsulated nanoparticles were then exposed to buffers at two different values of pH: one at physiological (pH 7.4) and the other at pH 5.5 (Figure 4 C). Release of doxorubicin was monitored through changes in absorbance values of the drug in the supernatant buffer system over time. Only 17% release of doxorubicin was observed in first three hours at the physiological pH 7.4, while 100% release of doxorubicin was encountered within the same time period at pH 5.5. This observation confirms utility of these materials as stimuli responsive drug delivery vehicles under slightly acidic environments such as those found for tumors and bacterial infections. Such pH responsive drug release characteristics should allow localized delivery of therapeutic agents and thus minimize problematic side effects.

In order to evaluate pH responsive performance in an actual cellular environment, the cytotoxicity of the doxorubicin loaded nanoparticles were measured against a breast cancer cell line (MDA-MB 231) and were compared to cytotoxicities for a normal breast cell line

(HS578Bst) (Figures 4 A & B). Both cell lines were incubated with drug free and doxorubicin loaded [Ptc][DC] nanoparticles for 48 hours and cell viabilities were determined. It was observed that normal breast cells remained essentially unaffected by both drug free and doxorubicin loaded nanoparticles with increasing concentrations of the nanoparticles. However, with breast cancer cell lines a concentration dependent cell death was observed with doxorubicin loaded nanoparticles demonstrating 37% cell viability at the highest concentration studied (48 μ M). In contrast, drug free [Ptc][DC] nanoparticles did not significantly inhibit cell proliferation even at the highest concentrations (100 μ M), indicating their high non-cytotoxic properties. Existing literature³⁰ indicates two possible mechanism of action for the widely studied chemotherapeutic drug doxorubicin. The drug is known either to intercalate with DNA thereby disrupting topoisomerase-II mediated DNA repair or they generate free radicals that damages the cell membrane, proteins as well as DNA leading to cell death. In the present study, the confocal fluorescence microscopy image (Fig. 4D) does not suggest the presence of [Ptc][DC] nanoparticles in the nucleus. Therefore cell death is primarily assumed to be a result of cellular membrane damage. Since the extracellular pH of the cancer cell is more acidic the drug is released in the vicinity of the cell membrane unlike normal cells. This explains how the doxorubicin loaded PtcDC nanoparticles can selectively destroy cancer cells leaving the normal cells unaffected. Thus, these observations indicate that this novel and simplistic approach to developing multifunctional pH sensitive nanoparticles may be used for stimuli responsive drug delivery to acidic environments such as cancer cells and infected tissues. The inherent biocompatibility observed for these nanomaterials exclude the need for inducing biocompatibility through conjugation with more compatible polymers or proteins. In addition, confocal fluorescence microscopic images (Figure 4D) obtained for the MDA-MB-231 cell line,

after 2 hrs incubation with drug free [Ptc][DC] nanoparticles, clearly suggests the potential of these nanoparticles for use in simultaneous imaging and therapy. Since deoxycholate is non-fluorescent, the observed fluorescence was attributed to the phthalocyanine counterpart, thereby establishing actual capability of these materials for combined therapy and diagnosis. Most current multimodal theranostic approaches involve conjugation of separate moieties for each functionality, thereby leading to highly elongated synthetic procedures.¹⁻³ Therefore, a one-pot synthesis of a multifunctional theranostic materials, as reported in this study, significantly simplifies the synthetic methodology and thus yields a more affordable end product.

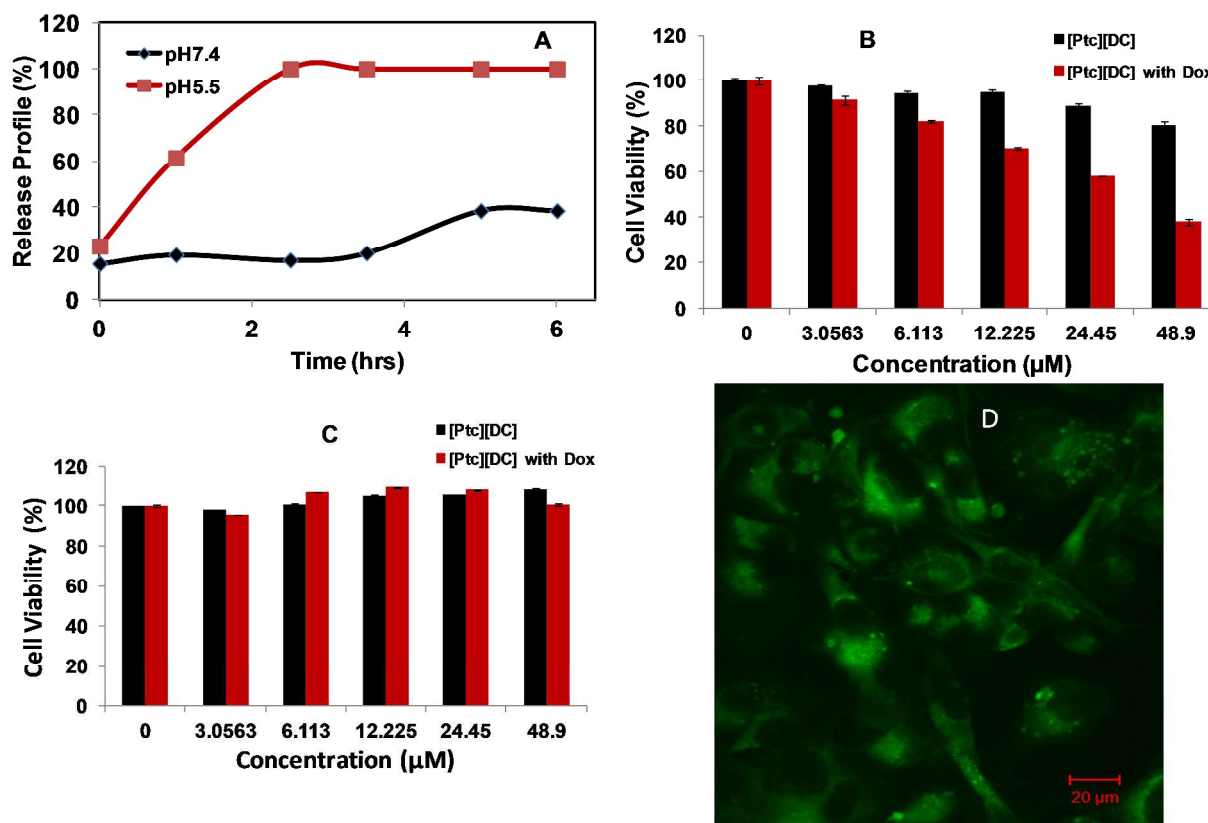


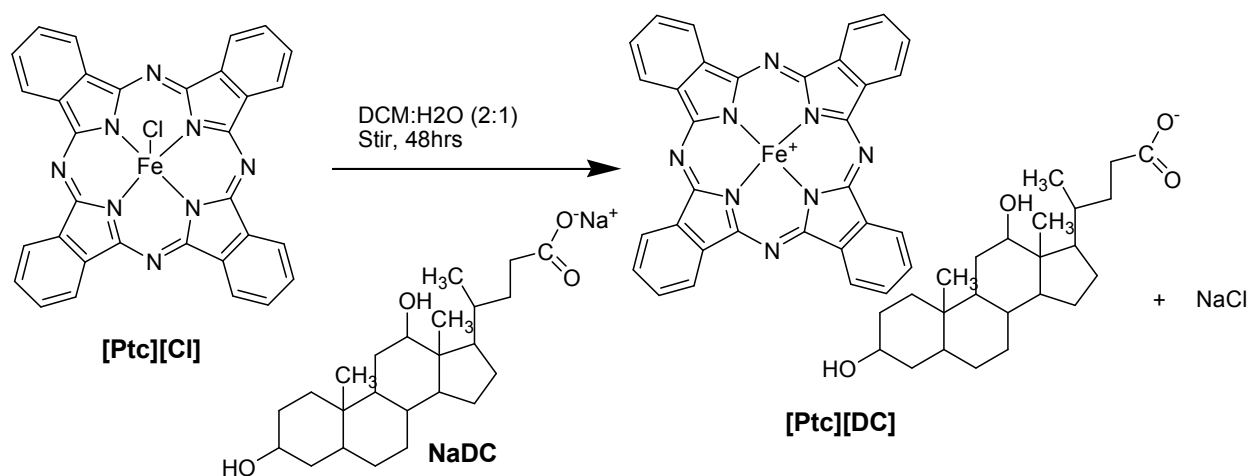
Figure 4: (A) Release profile of doxorubicin from [Ptc][DC] nanoparticles with varying pH. Cell viability studies of free [Ptc][DC] and doxorubicin loaded [Ptc][DC] nanoparticles in (B) Hs578Bst (normal breast) and (C) MDA-MB-231 (breast cancer) cell lines (D) Confocal

microscopic image of MDA-MB 231 cells after 2 hrs incubation with Dox free [Ptc][Dc] nanoparticles.

Experimental Section

Synthesis of [Ptc][DC]

A biphasic ion-metathesis reaction was performed by use of dark green phthalocyanine iron(III) chloride ([Ptc][Cl]) dissolved in dichloromethane (DCM) and sodium deoxycholate (NaDC) dissolved in water to achieve a 1:1.1 ratio mixture which was stirred for 48 hours (Scheme 1). The resulting salt [Ptc][DC] which was soluble in DCM, was then separated from the aqueous phase and washed repeatedly with water to effectively remove the byproduct (NaCl), followed by lyophilization, yielding a blue solid (~92 % yield). The presence of both ions in the final product was confirmed by use of electrospray ionization (ESI) performed in both positive and negative ion modes [(MS, ESI⁺) m/z 568 (MS, ESI⁻) m/z 338 (M- C₂H₂O₂), 320 (M- C₃H₄O₂)], FTIR (details in Supporting Information) (Figure S1) and ¹H NMR (details in Supporting Information).



Scheme 1: A schematic representation for synthesis of Iron(III)phthalocyanine based pH sensitive organic salt [Ptc][DC].

Synthesis of nanomaterials

The [Ptc][DC] nanoparticles were synthesized using a reprecipitation approach in which 100 μL of 1 mM stock of the compound in THF was injected into 5 mL of phosphate buffer at pH 7.4 under sonication, followed by aging of the nanoparticles for one-half hour before measurements.

Characterization of size and morphology of nanomaterials

TEM micrographs were obtained using an LVEM5 transmission electron microscope (DeLong America, Montreal, Canada). Nanoparticle dispersions (3 μL) were drop casted onto a carbon coated copper grid and allowed to dry in air at room temperature before TEM imaging.

Absorption and fluorescence studies

Absorbance measurements were performed on a Shimadzu UV- 3101PC, a UV-Vis-near-IR scanning spectrometer (Shimadzu, Columbia, MD). Fluorescence studies were performed using a Spex Fluorolog-3 spectrofluorimeter (model FL3-22TAU3); Jobin Yvon, Edison, NJ). A 0.4 cm path length quartz cuvette (Starna Cells) was used for acquiring fluorescence and absorbance data against an identical cell filled with pure water as blank. Fluorescence studies were performed using right angle geometry. The fluorescence quantum yield of the [Ptc][DC] nanoparticles were measured using a relative approach³¹ using disodium fluorescein in 0.1 N NaOH (quantum yield=0.93) as standard and an excitation wavelength of 400 nm.

For confocal microscopy, cells were incubated with test compounds at a final concentration of 20 μM for 2 h. Cell images were acquired using a (x40) objective with a confocal laser microscope (Zeiss 510 confocal microscope) equipped with an argon laser for excitation at 488 nm.

Magnetic property measurement

Magnetic properties of the bulk material and the lyophilized nanoparticles were studied using Magnetic Property Measurement System (*Quantum Design*). Field scans (-7 T to +7 T) at a given temperature and temperature scans (0 to 300 K) at a given field were both performed.

Drug Encapsulation in nanoparticles

Four (4) mg of doxorubicin were dissolved into 10 mL of water (pH 8) to achieve a final concentration of 0.4 mg/mL, followed by injection of 200 μL of 1 mM [Ptc][DC] stock in THF into this volume under sonication to form nanoparticles. Nanoparticles with the given drug were sonicated for 30 min and then allowed to stand for 24 h to allow diffusion into the nanoparticles and equilibration. Due to hydrophobic characteristics of the drug as well as pi-pi interactions between the drug and phthalocyanine molecules, the drug is assumed to be mostly encapsulated within the phthalocyanine nanoparticles. These drug loaded nanoparticles were then centrifuged at 2000 rpm for 20 min and the supernatant was separated from the pellet. The nanoparticles were then lyophilized and drug delivery was studied using variations in pH environments. The stock doxorubicin without nanoparticles was also studied under similar conditions. Doxorubicin stock solution without nanoparticles was prepared at the same time as preparation of nanoparticles, sonicated and allowed to stand for 24 h, after which the absorbance was measured and compared to the absorbance of doxorubicin in the supernatant in order to determine the

amount of drug encapsulated. Incubation of 20 μM nanoparticles with 0.4 mg/mL of doxorubicin for 24 h led to encapsulation of 0.07 mg/mL of the drug which amounts to 17 % drug encapsulation and 33% drug loading efficiency of the particles. The amount of drug encapsulated was obtained by subtracting the amount of drug remaining in the supernatant of the centrifuged drug loaded nanoparticles from the total amount of drug taken using absorbance measurements. Drug free bare nanoparticles were similarly prepared, centrifuged, lyophilized and weighed for obtaining the drug loading efficiency of the particles.

Cell Studies

Cytotoxicities of the synthesized drug free and drug loaded nanomaterials were determined against breast cancer (MDA-MB-231, ATCC no. HTB-26) and normal breast (Hs578Bst, ATCC no. HTB-125) cell lines by use of MTT Assay kit (Promega Corporation, Madison, WI, USA), according to the manufacturer's instructions. Briefly, in a 96-well plate, 5000 cells in 0.1 mL culture medium were seeded to each well. After 24 h, the old culture medium was removed and discarded. Then, 0.1 mL of new culture medium containing 0-40 μM of salts were dissolved in 1% DMSO and introduced to the cells. Cells were then incubated for 48 h at 37 $^{\circ}\text{C}$, under a 5% CO_2 atmosphere. At the end of the incubation period, cells were treated with 15 μL 3-(4,5-dimethylthiazol-2-yl)-2,5-diphenyltetrazolium bromide (MTT) and incubated for 2 h. After 2 h, 100 μL of the stock solution was added per well and incubated overnight. The plate was shaken for 20 sec and absorbance read at 570 nm with a reference wavelength of 650 nm using a micro plate spectrophotometer (Benchmark Plus, Bio-Rad Laboratories, Hercules, CA, USA). Cell viability as a percentage was determined by taking the ratio between absorbance of the treated cells and absorbance of untreated (control) cells taken as 100%.

Conclusions

In summary, this study reports a facile one-pot approach for syntheses of pH responsive-magnetic-fluorescent organic salts by use of ionic liquid chemistry. Nanoparticles obtained through a one-step reprecipitation approach demonstrated extremely interesting multimodal properties which are suitable for combined imaging and targeted stimuli responsive release of therapeutic agents. These materials demonstrate nearly 100% cell viability at all concentrations for normal and cancer cells studied, suggesting its fairly low cytotoxicity. The *in-vitro* pH responsive drug delivery properties of these nanomaterials in actual cellular environment could be efficiently used for selective delivery of therapeutic agents directly to tumors and other acidic environments. In addition, the observed interesting transition in magnetic properties, which allowed switching from a diamagnetic bulk material to paramagnetic nanoparticles signifies potential applications for targeted drug delivery using an external magnetic field and magnetic hyperthermia. Confocal fluorescence microscopic images obtained for MDA-MB-231 cell lines after short incubation with [Ptc][DC] nanoparticles suggests its use for simultaneous fluorescence imaging and therapy. Thus, these highly biocompatible theranostic nanoparticles should be extremely promising as stimuli responsive drug delivery systems. Finally, the facile synthetic strategy demonstrated in this study for development of these new and improved multifunctional nanoparticles emphasizes on the simplistic design of materials for personalized theranostic treatments.

Acknowledgements

IMW acknowledges financial support from the National Science Foundation (grant number CHE-130761). The authors also acknowledge the Pennington Biomedical Research

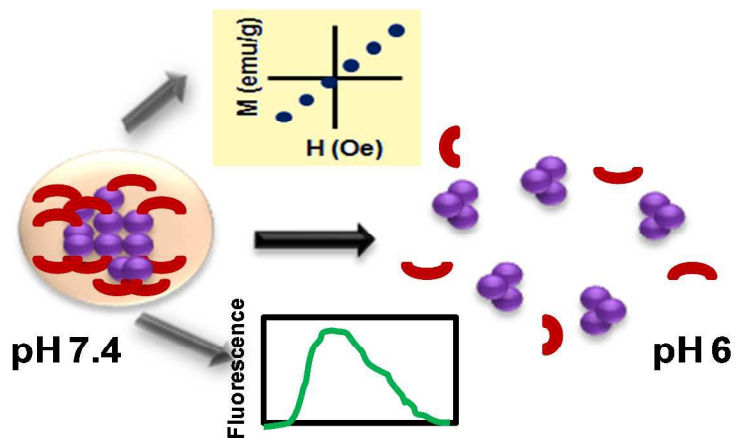
Center for allowing use of their confocal microscopy facility and Dr. David Burk for technical assistance with this equipment.

Notes and References

1. S. S. Kelkar and T. M. Reineke, *Bioconjugate Chemistry*, 2011, **22**, 1879-1903.
2. M. Ferrari, *Nature Reviews Cancer*, 2005, **5**, 161-171.
3. M. E. Caldorera-Moore, W. B. Liechty and N. A. Peppas, *Accounts of Chemical Research*, 2011, **44**, 1061-1070.
4. C. Caltagirone, A. M. Falchi, S. Lampis, V. Lippolis, V. Meli, M. Monduzzi, L. Prodi, J. Schmidt, M. Sgarzi, Y. Talmon, R. Bizzarri and S. Murgia, *Langmuir*, 2014, **30**, 6228-6236.
5. F. Alexis, E. Pridgen, L. K. Molnar and O. C. Farokhzad, *Molecular Pharmaceutics*, 2008, **5**, 505-515.
6. Z. Cheng, A. Al Zaki, J. Z. Hui, V. R. Muzykantov and A. Tsourkas, *Science (Washington, DC, United States)*, 2012, **338**, 903-910.
7. X. Tan, L. Feng, J. Zhang, K. Yang, S. Zhang, Z. Liu and R. Peng, *ACS Applied Materials & Interfaces*, 2013, **5**, 1370-1377.
8. J. Jeong, E.-K. Kwon, T.-C. Cheong, H. Park, N.-H. Cho and W. Kim, *ACS Applied Materials & Interfaces*, 2014, **6**, 5297-5307.
9. S. Mazzucchelli, M. Colombo, C. De Palma, A. Salvade, P. Verderio, M. D. Coghi, E. Clementi, P. Tortora, F. Corsi and D. Prospero, *ACS Nano*, 2010, **4**, 5693-5702.
10. J. E. Smith, K. E. Sapsford, W. Tan and F. S. Ligler, *Analytical Biochemistry*, 2011, **410**, 124-132.
11. J. H. Choi, F. T. Nguyen, P. W. Barone, D. A. Heller, A. E. Moll, D. Patel, S. A. Boppart and M. S. Strano, *Nano Letters*, 2007, **7**, 861-867.
12. W. J. M. Mulder, R. Koole, R. J. Brandwijk, G. Storm, P. T. K. Chin, G. J. Strijkers, C. de Donega, K. Nicolay and A. W. Griffioen, *Nano Letters*, 2006, **6**, 1-6.
13. G. H. Gao, G. H. Im, M. S. Kim, J. W. Lee, J. Yang, H. Jeon, J. H. Lee and D. S. Lee, *Small*, 2010, **6**, 1201-1204.
14. M. Das, D. Mishra, P. Dhak, S. Gupta, T. K. Maiti, A. Basak and P. Pramanik, *Small*, 2009, **5**, 2883-2893.
15. S. Santra, C. Kaittanis, J. Grimm and J. M. Perez, *Small*, 2009, **5**, 1862-1868.
16. H. Yoo, S.-K. Moon, T. Hwang, Y. S. Kim, J.-H. Kim, S.-W. Choi and J. H. Kim, *Langmuir*, 2013, **29**, 5962-5967.
17. S.-h. Xuan, S.-F. Lee, J. T.-F. Lau, X. Zhu, Y.-X. J. Wang, F. Wang, J. M. Y. Lai, K. W. Y. Sham, P.-C. Lo, J. C. Yu, C. H. K. Cheng and K. C.-F. Leung, *ACS Applied Materials & Interfaces*, 2012, **4**, 2033-2040.
18. S. Liu, X. Jiang and G. Zhuo, *New Journal of Chemistry*, 2007, **31**, 916-920.
19. B. Koo, H. Baek and J. Cho, *Chemistry of Materials*, 2012, **24**, 1091-1099.
20. T. Nyokong and E. Antunes, *Coordination Chemistry Reviews*, 2013, **257**, 2401-2418.
21. L. H. Reddy, J. L. Arias, J. Nicolas and P. Couvreur, *Chemical Reviews (Washington, DC, United States)*, 2012, **112**, 5818-5878.

22. N. Nasongkla, E. Bey, J. Ren, H. Ai, C. Khemtong, J. S. Guthi, S.-F. Chin, A. D. Sherry, D. A. Boothman and J. Gao, *Nano Letters*, 2006, **6**, 2427-2430.
23. Y.-w. Jun, Y.-M. Huh, J.-s. Choi, J.-H. Lee, H.-T. Song, S. Kim, S. Yoon, K.-S. Kim, J.-S. Shin, J.-S. Suh and J. Cheon, *Journal of the American Chemical Society*, 2005, **127**, 5732-5733.
24. A. Rich and D. M. Blow, *Nature (London, United Kingdom)*, 1958, **182**, 423-426.
25. I. K. Kandela, W. Lee and G. L. Indig, *Biotechnic & Histochemistry*, 2003, **78**, 157-169.
26. F. Sonvico, S. Mornet, S. Vasseur, C. Dubernet, D. Jaillard, J. Degrouard, J. Hoebeke, E. Duguet, P. Colombo and P. Couvreur, *Bioconjugate Chemistry*, 2005, **16**, 1181-1188.
27. P. H. Mutin, G. Guerrero and A. Vioux, *Journal of Materials Chemistry*, 2005, **15**, 3761-3768.
28. K. Sakamoto and E. Ohno-Okumura, *Materials*, 2009, **2**, 1127-1179.
29. C. Balraj and K. P. Elango, *Spectrochimica Acta, Part A: Molecular and Biomolecular Spectroscopy*, 2012, **86**, 44-50.
30. C. F. Thorn, C. Oshiro, S. Marsh, T. Hernandez-Boussard, H. McLeod, T. E. Klein and R. B. Altman, *Pharmacogenet Genomics.*, 2011, **21(7)**, 440-446.
31. Albrecht, C., *Principles of fluorescence spectroscopy, 3rd Edition, Joseph R. Lakowicz, editor.* 2008; Vol. 390, p 1223-1224.

Graphical Abstract



This study represents a one pot simplistic approach towards development of multimodal theranostic nanomaterials.